

## DTA–GC–MS coupling for the characterization of the volatile products resulting from the decomposition of organic templates occluded in zeolites<sup>1</sup>

M. Soulard, S. Bilger, H. Kessler and J.L. Guth

*Laboratoire de Matériaux Minéraux, URA CNRS 428, Ecole Supérieure de Chimie de Mulhouse, 3 rue Alfred Werner, 68093 Mulhouse Cedex (France).*

(Received 2 September 1991; in final form 17 December 1991)

### Abstract

The volatile products resulting from the thermal degradation, in an inert atmosphere, of tetrapropylammonium cations, occurring as templates in MFI-type zeolites were analysed at first by means of a set-up coupling the DTA and MS techniques. Next, in order to make their identification easier, the various constituents of the gaseous mixture, evolving from the thermoanalyser, were separated through a chromatographic column before they entered the mass spectrometer. These combined techniques (DTA–GC–MS), revealed the presence of significant amounts of propene during the different stages of decomposition. This suggests for the initial decomposition mechanism a Hofmann elimination reaction followed by  $\beta$ -eliminations. In addition to propene and its oligomers, a variety of hydrocarbons (alkanes, alkenes, aromatics) are evolved. Their nature and proportions depend among others on the temperature and on the acidity of the zeolite. Thus, the main decomposition is accompanied by various secondary reactions due to the catalytic effect of these materials. This coupling of techniques appears as an effective tool to elucidate the complicated process of this type of degradation.

### INTRODUCTION

Zeolites are obtained by hydrothermal crystallization from alkaline [1] or fluoride-containing [2] mixtures in the presence of various templates such as tetrapropylammonium cations ( $\text{Pr}_4\text{N}^+$ ). The chief role of these organic species is a structure-directing one and the zeolitic framework is built around them. After synthesis, they are occluded inside the channels of the zeolites and may occur in the solid in various forms: as ion pairs  $\text{Pr}_4\text{N}^+\text{OH}^-$  or  $\text{Pr}_4\text{N}^+\text{F}^-$ ; as lone  $\text{Pr}_4\text{N}^+$  counteracting the negative charge of the

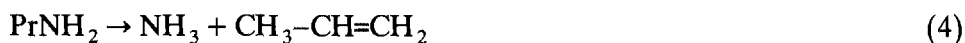
---

*Correspondence to:* M. Soulard, Laboratoire de Matériaux Minéraux, URA CNRS 428, Ecole Supérieure de Chimie de Mulhouse, 3 rue Alfred Werner, 68093 Mulhouse Cedex, France.

<sup>1</sup> This paper was presented during the 22nd annual meeting of the French Association of Calorimetry and Thermal Analysis (AFCAT) at Paris-XI–Châtenay-Malabry (27–29 May 1991).

three-dimensional lattice of tetrahedra, when part of Si(IV) is substituted by a T(III) element such as aluminium; as cations associated with lattice defects and characterized by  $\text{>Si-O}^- \text{Pr}_4\text{N}^+$  interactions.

Turning the samples into catalytically active substances requires the removal of the organic matter, usually by thermal degradation. By means of thermoanalytical methods (DTA, TG, DSC), MFI-type zeolites were characterized [3,4] especially as a function of the Si/T(III) ratio, by investigation of the thermal decomposition of the templates. IR and  $^{13}\text{C}$  CP-MAS NMR spectrometry were applied to the as-synthesized samples (precursors) and after heating them, in order to identify the products remaining in the solid after partial degradation of the templates [5]. It was shown that, in a first step,  $\text{Pr}_4\text{N}^+$  incorporated in MFI-type zeolites is transformed into  $\text{Pr}_3\text{NH}^+$  and  $\text{Pr}_3\text{N}$  species. In the following ones, the presence of  $\text{Pr}_2\text{NH}$  and  $\text{Pr}_2\text{NH}_2$  suggested a stagewise degradation involving a Hofmann-type reaction, followed by successive  $\beta$ -eliminations, according to the four-stage scheme



where X = OH, F.

Towards the end of the degradation, the complex NMR spectra reveal the presence of a number of hydrocarbons resulting from the catalytic properties of these materials. In order to investigate this effect and to characterize the volatile compounds evolved during the decomposition of the templates, several coupled analytical techniques were used. At first, the volatiles were analysed by using a set-up coupling DTA and MS. Then, in a second type of experiment, the products released during the DTA were separated by gas chromatography before entering the spectrometer.

In this paper is reported the study of the thermal decomposition of tetrapropylammonium species occluded in three precursors. Two highly siliceous samples A ( $\text{Pr}_4\text{NF-MFI}$ ) and B ( $\text{Pr}_4\text{NOH-MFI}$ ) were prepared respectively in fluoride and in alkaline medium. Sample C ( $\text{Pr}_4\text{NF-(Si,Al)MFI}$ ) is an aluminium-containing material with a Si/Al molar ratio of 11.

## EXPERIMENTAL

### *Differential thermal analysis*

The experiments were performed by using a BDL-SETARAM model M2 differential thermal microanalyser, in an open platinum crucible, with a

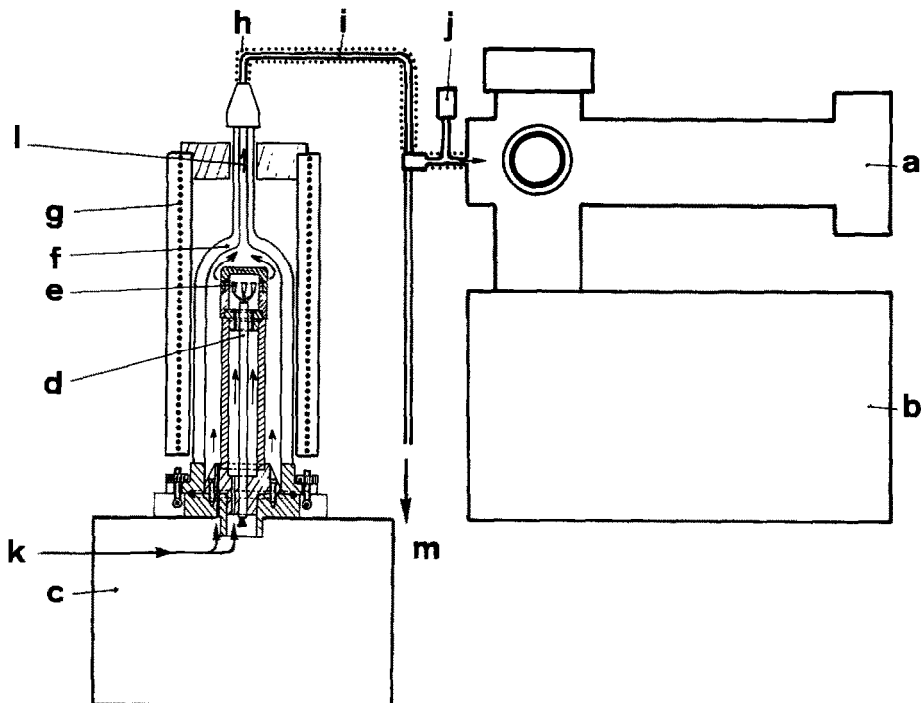


Fig. 1. Scheme of the DTA-MS coupling: (a) mass spectrometer, (b) pumping system, (c) temperature programmer, (d) DTA probe, (e) sample, (f) alumina sheath, (g) furnace, (h) heating ribbon, (i) connection tubing, (j) leak valve, (k) helium inlet, (l) gas to be analysed, (m) gas outlet.

heating rate of  $10^{\circ}\text{C min}^{-1}$ . The simple DTA measurements were carried out in an argon flow-rate of  $0.3 \text{ dm}^3 \text{ h}^{-1}$ , but a helium flow-rate of  $4 \text{ dm}^3 \text{ h}^{-1}$  was used for combined DTA-MS and DTA-GC-MS measurements.

### *Mass spectrometry*

The apparatus used was a NERMAG, type R.10.10 quadrupolar mass spectrometer. The spectra were recorded with a mass exploration from 10 to 250 u, performed for 0.5 s. The waiting time between two scans was 6 s and the ionization energy was 70 eV.

### *Coupling of the techniques*

For the simultaneous DTA-MS measurements, the set-up is given in Fig. 1. The thermoanalyser included an alumina sheath lengthened by a tube above the sample. The latter was connected to the mass spectrometer by a 0.8 m long 2 mm ID stainless steel pipe. This tubing was heated at about  $150^{\circ}\text{C}$  throughout its length to prevent the decomposition products

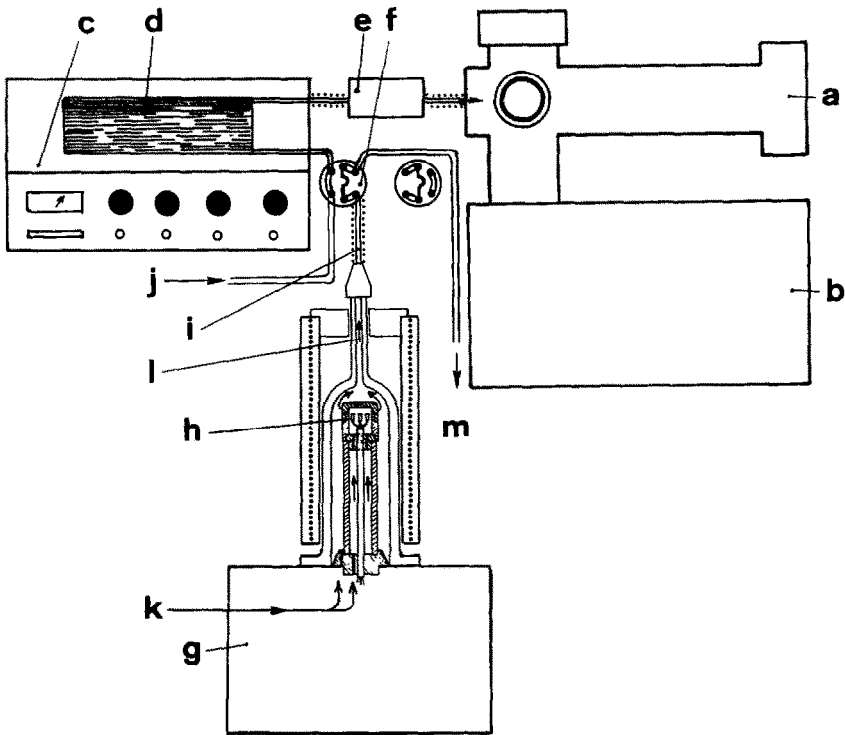


Fig. 2. Scheme of the DTA–GC–MS coupling: (a) mass spectrometer, (b) pumping system, (c) chromatograph, (d) capillary column, (e) interface, (f) injection valve, (g) temperature programmer, (h) DTA probe, (i) connection tubing, (j) carrier gas, (k) helium inlet, (l) gas to be analysed, (m) gas outlet.

from condensing. The helium carrier gas coming out of the DTA apparatus and containing the evolved volatiles, was divided into two parts: a small proportion of the gas flow was sampled continually into the mass spectrometer through a leak valve and the remaining part of this flow was discarded. The experimental data were processed in several ways. For a selected temperature, the mass spectrum corresponding to the whole set of species produced was determined. In addition, the ion signal change relevant to a given  $m/z$  fragment, as well as the total ion signal, were plotted against time or temperature. The spectra obtained correspond however to mixtures of species and in order to make their identification easier, a second set-up including a chromatograph was used.

For the combined DTA–GC–MS analyses (Fig. 2), the thermoanalyser was connected by the above-mentioned stainless steel tubing to a six-port injection valve with an external loop, on a DELSI 700 chromatograph. The interface between the chromatograph and the mass spectrometer was supplied by the manufacturer. The species were separated by means of two different types of capillary columns made of fused silica. A CHROMPACK

type  $\text{Al}_2\text{O}_3/\text{KCl}$ -PLOT (50 m  $\times$  0.32 mm) column was applied to the separation of light hydrocarbons ( $\text{C}_1$ – $\text{C}_{10}$ ) and a CHROMPACK type CP-Sil 5 CB-WCOT (50 m  $\times$  0.32 mm) column was suited to the separation of amines and hydrocarbons. The separation of the products was carried out by programming the temperature from 50 to 200°C with a heating rate of 3°C min<sup>-1</sup> when the chromatograph was equipped with the first column and of 4°C min<sup>-1</sup> with the second one. For a given temperature of decomposition, corresponding to a characteristic point of the DTA curve (minimum of the peak), this coupling of techniques allowed a preliminary separation of the volatile products issuing from the thermoanalyser, before they entered the spectrometer. Integration of the ion signal peak for each compound detected made it possible to obtain area percentages which represent roughly the weight composition of the gas mixture. The quantitative determination was not performed because it would have required a complete calibration with standards of each species present.

## RESULTS AND DISCUSSION

### *Thermal analysis*

Figure 3 shows the DTA and TG recordings of the three zeolitic precursors studied. For the  $\text{Pr}_4\text{NF}$ -MFI sample, the decomposition takes place in two temperature ranges (Fig. 3(a)). After a small endothermal shoulder, the DTA curve exhibits a first strong peak at 430°C, followed by a second, broader one, displaying a shoulder and a minimum around 534°C. The <sup>13</sup>C NMR study made it possible to ascribe the first peak to the transformation of  $\text{Pr}_4\text{N}^+$  into  $\text{Pr}_3\text{NH}^+$ , and the second one to the overall degradation of this last species. For the  $\text{Pr}_4\text{NOH}$ -MFI precursor, the decomposition begins 45°C lower (Fig. 3(b)). It results in a broad DTA endotherm with a minimum around 385°C, preceded by a weak shoulder and followed by two humps. The second hump, near 460°C, was assigned to the  $\text{Pr}_4\text{N}^+$  resulting from crystal defects. In the aluminium-containing precursor, the  $\text{Pr}_4\text{N}^+$  template appears predominantly as a compensation cation balancing the negative charge of the lattice. In this form  $\text{Pr}_4\text{N}^+$  is bonded to the framework by stronger interactions and its degradation starts at a higher temperature. Thus, the TG recording of this sample (Fig. 3(c)) reveals only one weight loss and the DTA curve exhibits a single peak with a minimum around 482°C.

### *DTA-MS coupled measurements*

Figure 4 shows the modification of the overall ionic current obtained for the decomposition products of the various precursors, as a function of temperature. The intensity of the ion signals passes through maxima

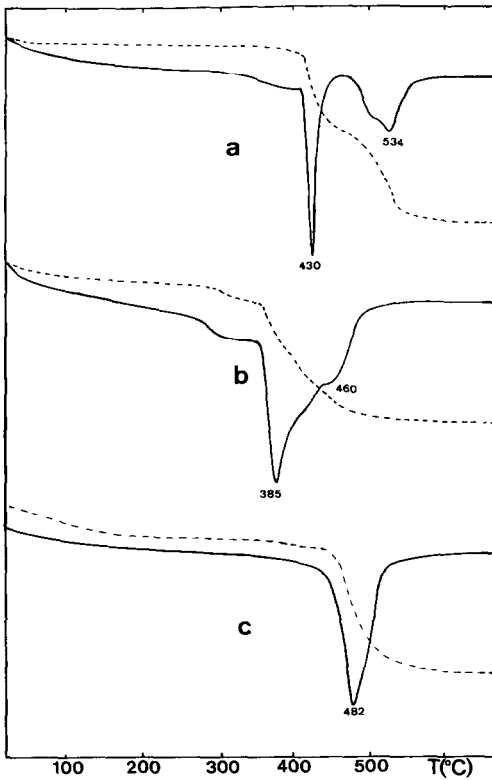


Fig. 3. Thermal analysis curves for the decomposition of the precursors in an inert gas flow: curve a,  $\text{Pr}_4\text{NF-MFI}$ ; curve b,  $\text{Pr}_4\text{NOH-MFI}$ ; curve c,  $\text{Pr}_4\text{NF-(Si,Al)MFI}$ ; —, DTA curve, — — —, TG curve.

corresponding to the endothermal peaks recorded by DTA and, therefore, the thermal effects observed are related to the generation of volatile species. The mass spectra (Fig. 5), recorded at the maximum ionic current, show a great number of lines because they correspond to mixtures of species, but with a fairly high number of similarities irrespective of the sample, because these are due to numerous common products. These spectra are also like those reported by Parker et al. [6] for a silicalite precursor. An identification was attempted by starting from the tables of published mass spectra [7].

On the spectrum relevant to the  $\text{Pr}_4\text{NF-MFI}$  precursor (Fig. 5(a)), recorded at 430°C (maximum of the first peak), series of lines appear among others, in the ranges 17–18, 26–30, 39–44, 55–58 and 67–72 and at 84 u. It follows therefore that propene, essentially represented by the ion signal at  $m/z$  41, is the major compound present. Other species are also detected; propane, partly represented by the  $m/z$  29 fragment and various hexene isomers, characterized by  $m/z$  55 and 84, resulting from the

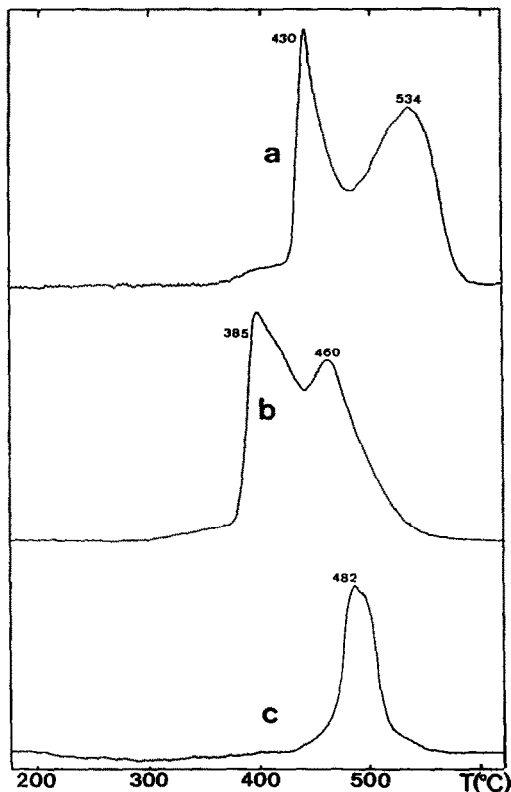


Fig. 4. Total ionic current vs. temperature for the volatile products evolved during the decomposition of the precursors by DTA-MS coupling: curve a,  $\text{Pr}_4\text{NF-MFI}$ ; curve b,  $\text{Pr}_4\text{NOH-MFI}$ ; curve c,  $\text{Pr}_4\text{NF-(Si,Al)MFI}$ .

dimerization of propene. Dimerization would proceed by the intermediate formation of carbenium ions followed by hydride transfer reactions [8]. In comparison with the previous spectrum, that (Fig. 5(a')) recorded at 534°C (top of the second peak) reveals some variations in the positions and especially in the intensities of the lines. While the content of propene decreases, those of lighter compounds such as ethene and ethane ( $m/z$  28) increase significantly, and those of heavier products ( $m/z$  70, 56, 43, ...) become noticeable. Lines with  $m/z$  30, 72 and 101 also reveal the presence of amines, especially dipropylamine.

For the  $\text{Pr}_4\text{NOH-MFI}$  precursor, the mass spectra recorded at the two maxima of the ion signals (Fig. 5(b) and (b')) are similar to the previous ones, thus revealing that the volatile compounds resulting from the decomposition are slightly affected by the nature of the anion. Yet, the first peak to the degradation of  $\text{Pr}_4\text{NOH}$  corresponds to a larger amount of propene than in the previous case and the content of  $\text{C}_6\text{H}_{12}$  dimers becomes lower.

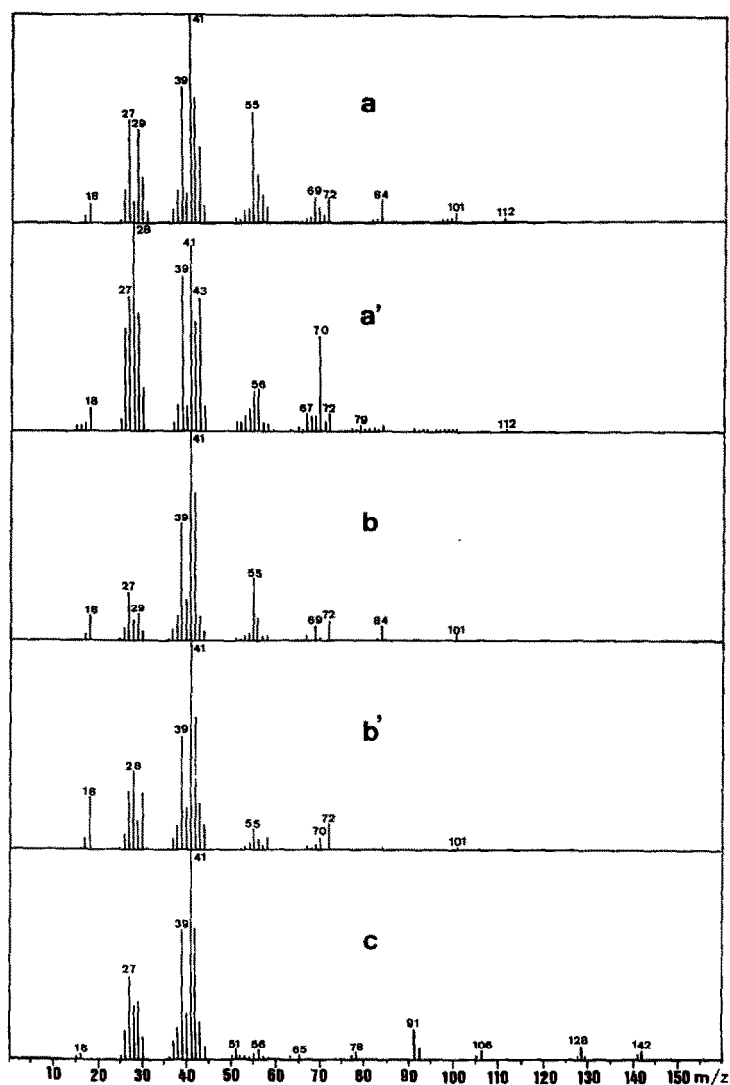


Fig. 5. Mass spectra of the volatile decomposition products, recorded at the maxima of the ionic currents by DTA-MS coupling: (a) top of the first peak (430°C) and (a') top of the second peak (534°C) of  $\text{Pr}_4\text{NF-MFI}$ ; (b) top of the first peak (385°C) and (b') top of the second peak (460°C) of  $\text{Pr}_4\text{NOH-MFI}$ ; (c)  $\text{Pr}_4\text{NF-(Si,Al)MFI}$  at 482°C.

In contrast the second part of the  $\text{Pr}_4\text{NOH}$  decomposition yields lower amounts of light hydrocarbons ( $\text{C}_2$ ) and also of heavier products.

In addition to lines assigned to propene and propane, the mass spectrum corresponding to the aluminium-containing sample (Fig. 5(c)) exhibits extra lines, relevant to molecular ions ( $m/z$  91, 106, 128, 142) and representative of toluene, xylene, naphthalene and methylnaphthalene, respectively. The



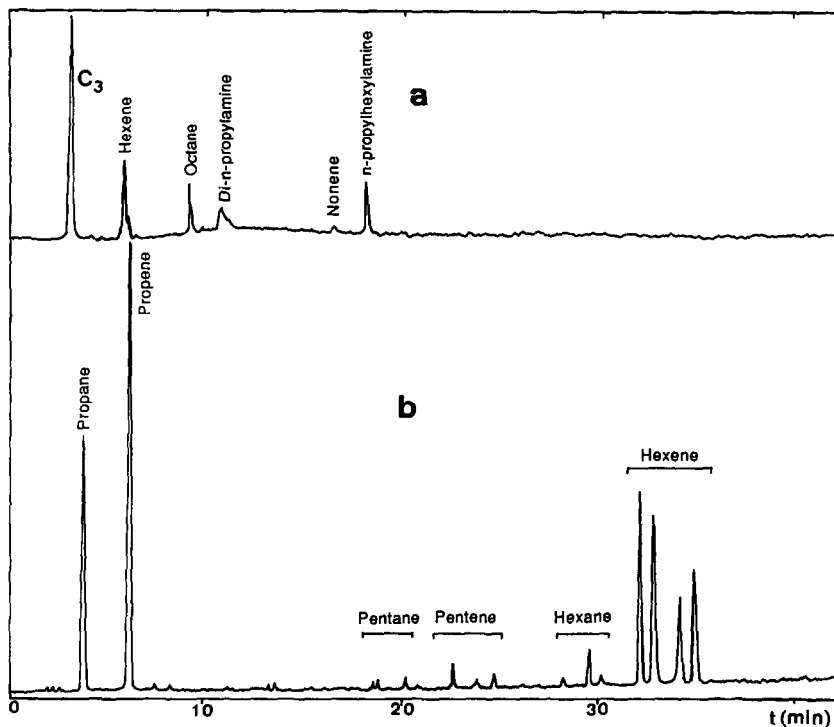


Fig. 6. Chromatograms of the gas mixture resulting from the decomposition of the  $Pr_4NF$ -MFI precursor at the first peak by DTA-GC-MS coupling: (a) separation with the CP-Sil 5 CB-WCOT column; (b) separation with the  $Al_2O_3$ /KCl-PLOT column.

presence of aromatics thus provides evidence for an acid catalyst related to this sample.

#### *DTA-GC-MS simultaneous measurements*

Identification of some products, especially minor species, from the mass spectra obtained by a simple DTA-MS coupling is rather critical. Therefore, the study was completed by using the DTA-GC-MS set-up. Chromatographic separation provides quantitative information and makes the interpretation easier. For instance, Figs. 6 and 7 show the chromatograms obtained in using the two types of columns for the gas mixture produced by the degradation of the  $Pr_4NF$ -MFI precursor and the aluminium-containing sample, respectively. Table 1 shows the distribution of the decomposition products resulting from the three precursors investigated. The gas injections were carried out at the stated temperatures corresponding to the minima of the DTA peaks, in the 385–534°C range. The tabulated values

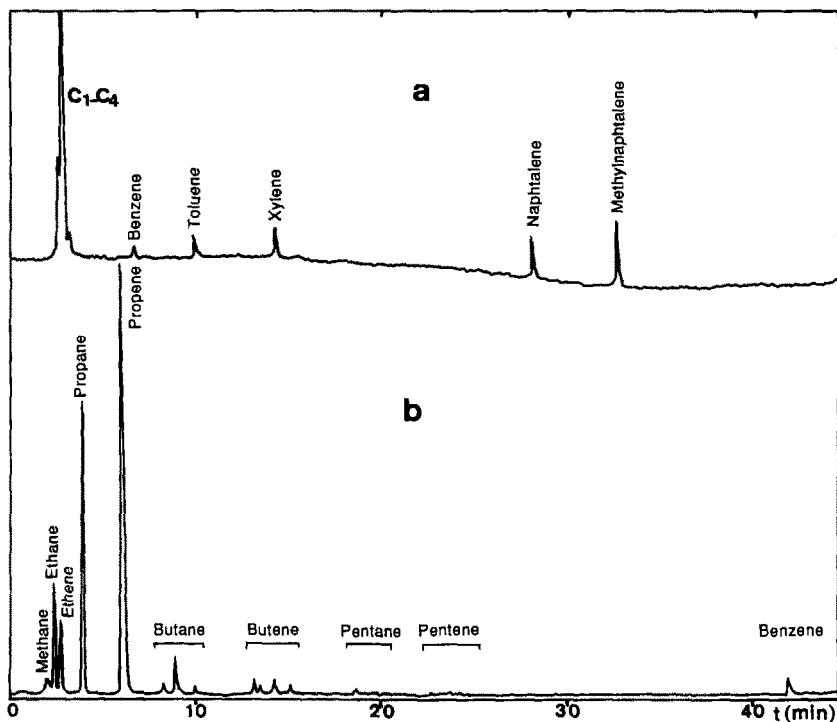


Fig. 7. Chromatograms of the gas mixture resulting from the decomposition of the  $\text{Pr}_4\text{NF}-(\text{Si},\text{Al})\text{MFI}$  precursor by DTA-GC-MS coupling: (a) separation with the CP-Sil 5 CB-WCOT column; (b) separation with the  $\text{Al}_2\text{O}_3/\text{KCl}$ -PLOT column.

are peak surface percentages of the total ionic current of the detected species. Circular diagrams (Fig. 8) enable one to compare the overall contents of alkanes, alkenes, aromatics and amines for each case.

#### *Highly siliceous samples*

At the first peak, in addition to significant amounts of propene and of dimers, low quantities of various hydrocarbons ( $\text{C}_2$ - $\text{C}_9$ ), noticeable proportions of *n*-propylamine, di-*n*-propylamine and also *n*-propylhexylamine were detected, excluding tri-*n*-propylamine. The presence of *n*-propylhexylamine would result from addition reactions between hexene and propylamine. At the second peak, one observed again relatively high amounts of propene but very low quantities of dimers, appreciably higher amounts of light hydrocarbons and also of heavier products ( $\text{C}_8$ ), such as 2-methyl-3-ethylpentane and 2,3-dimethylhexane. Some differences appeared between the two kinds of samples. They are presumably due to the nature of the anion ( $\text{OH}^-$  or  $\text{F}^-$ ) accompanying the organic cation and to the temperature of decomposition.

TABLE 1

Distribution of the decomposition products (percentage area)

	Pr <sub>4</sub> NOH-MFI (A)		Pr <sub>4</sub> NF-MFI (B)		Pr <sub>4</sub> NF- (Si,Al)MFI (C) 482°C
	430°C	534°C	385°C	460°C	
Methane + methylamine		7.18	2.01	2.41	0.12
Ethane		5.82	0.12	2.95	8.40
Ethene		14.98	0.06	0.59	4.46
Propane	12.81	18.78	2.92	2.88	17.18
Propene	39.57	16.15	60.45	72.81	50.72
<i>n</i> -Propylamine			1.01	0.13	
Butane					1.31
Butene		2.23	0.08	0.60	1.50
Pentane	0.05	0.24	0.08		0.11
Pentene	0.07	3.10	0.14	0.44	0.07
Di- <i>n</i> -propylamine	5.73	2.78	7.60	4.35	
Hexane	1.50	0.59			
Hexene	21.06	3.39	13.72	4.56	
Benzene					0.60
Toluene					1.07
Octane	5.79	20.79	4.25	6.43	
Xylene					1.52
<i>n</i> -Propylhexylamine	13.09	3.97	7.56	1.85	
Nonene	0.32				
Naphthalene					5.08
Methylnaphthalene					7.85

*Aluminium-containing sample*

Substitution of aluminium for silicon in the zeolitic framework has a marked effect on the nature of the decomposition products. For example, while no trace of amine is detected, a noteworthy yield of various aromatics is found. The latter may be accounted for by the acid character of the sample. For the mechanism of conversion of propene into aromatics, Poutsma [8] proposed a series of reactions involving Brönsted-acid centres as active sites.

## CONCLUSIONS

The DTA-MS combined techniques and mainly the DTA-GC-MS coupling, turn out to be effective tools to identify the numerous volatile products evolved during the thermal decomposition of the Pr<sub>4</sub>N<sup>+</sup> templates occluded in MFI-type zeolites. The constant presence of propene, which is the major primary degradation product, suggests an initial decomposition mechanism involving a Hofmann elimination reaction followed by  $\beta$ -eliminations. This simplified model, however, is supplemented by many

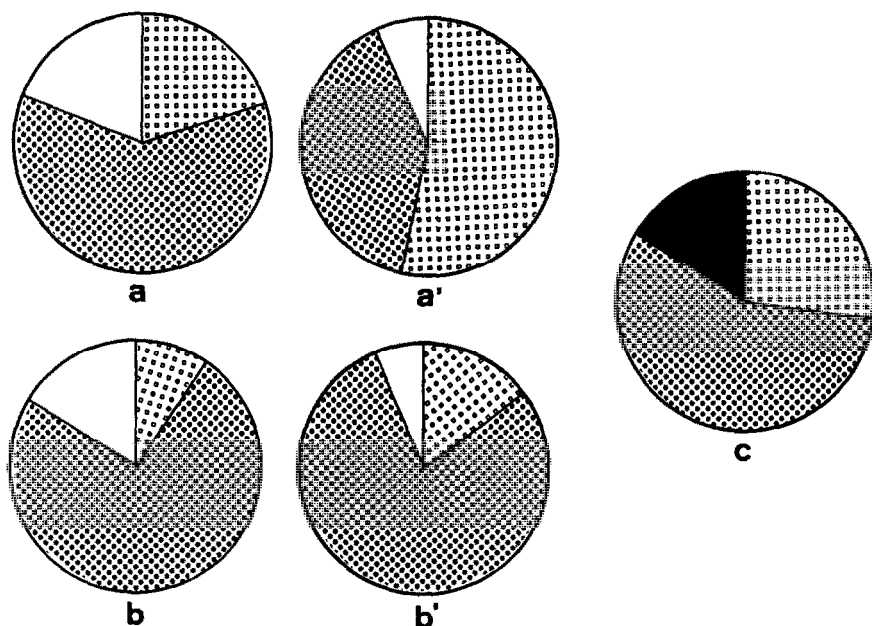






Fig. 8. Distribution diagrams of decomposition products (area %): (a) sample (A) at 430°C (top of the first peak); (a') sample (A) at 534°C (top of the second peak); (b) sample (B) at 385°C (top of the first peak); (b') sample (B) at 460°C (top of the second peak); (c) sample (C) at 482°C (top of the single peak);  alkanes,  alkenes,  amines,  aromatics.

other reactions, e.g. oligomerizations, cyclizations, hydrogen transfers, in which alkanes and aromatics are produced.

#### ACKNOWLEDGEMENT

The authors thank P. Wagner for skillful technical assistance with the mass spectrometry experiments.

#### REFERENCES

- 1 R.J. Argauer and G.R. Landolt, U.S. Patent 3,702,886, 1972.
- 2 J.L. Guth, H. Kessler and R. Wey, in Y. Murakami, A. Iijima and J.W. Ward (Eds.), Proc. 7th Int. Zeolites Conf., Tokyo, 1986, Elsevier, Amsterdam, 1986, p. 121.
- 3 M. Soulard, S. Bilger, H. Kessler and J.L. Guth, *Zeolites*, 7 (1987) 463.
- 4 M. Soulard, S. Bilger, H. Kessler and J.L. Guth, *Recueil des Actes des 18èmes Journées de Calorimétrie et d'Analyse Thermique*, Bordeaux, 1987, Ed. AFCAT, 1987, p. 141.
- 5 M. Soulard, S. Bilger, H. Kessler and J.L. Guth, *Zeolites*, 11 (1991) 107.
- 6 L.M. Parker, D.M. Bibby and J.E. Patterson, *Zeolites*, 4 (1984) 168.
- 7 *Eight Peak Index of Mass Spectra*, 2nd edn. Mass Spectrometry Data Centre, AWRE, Berkshire, UK, 1974.
- 8 M.L. Poutsma, *Zeolite Chemistry and Catalysis*, ACS Monogr., 171 (1976) 437.